
Article:
Zhu, Z.Q., Chen, Y.S. and Howe, D. (2000) Online optimal flux-weakening control of permanent-magnet brushless AC drives. IEEE Transactions on Industry Applications, 36 (5). pp. 1661-1668. ISSN 0093-9994

https://doi.org/10.1109/28.887219

Online Optimal Flux-Weakening Control of Permanent-Magnet Brushless AC Drives

Z. Q. Zhu, *Member, IEEE*, Y. S. Chen, and David Howe

***Abstract*—An enhanced online optimal control strategy, which maximizes the flux-weakening performance of a brushless ac motor, is described, and applied to motors having different rotor topologies: interior (radial or circumferential), inset, and surface-mounted magnet. It enables the maximum inherent power capability of a brushless ac motor to be achieved independent of any variation in its parameters, and facilitates maximum efficiency over the entire speed range. It also results in good transient dynamic performance, since it is coupled with feedforward vector control based on optimal current profiles.**

***Index Terms*—Brushless ac drive, flux weakening, optimal control, permanent-magnet machine.**

I. Introduction

VECTOR-CONTROLLED permanent-magnet brushless ac motors are used extensively for variable-speed applications, such as traction drives and machine tool spindle drives, for which both constant torque and constant power (flux weakening) modes of operation are required. In the constant torque mode, the phase currents can be controlled to optimize alternative performance criteria, such as the torque per ampere or the power factor [1]. In the flux-weakening mode, when the inverter voltage is limited, various control algorithms have been proposed to achieve the desired torque–speed performance [2]. The most common control schemes are feedforward, in which optimal profiles for the d- and q-axes currents, I_d^* and I_q^*, (asterisks designating demanded values) over the constant torque and flux-weakening operating ranges are derived from mathematical models, for which an accurate knowledge of the motor parameters is required [2]–[6].

The influence of the machine parameters on the performance of brushless ac motors has been investigated extensively [7], [8]. By way of example, however, Fig. 1(a) shows how the torque–speed characteristic of a brushless ac motor, having an interior radial magnet rotor (see the Appendix), varies with its back EMF, in each case the optimal I_d^* and I_q^* profiles for maximum torque capability being derived from a model of the motor which assumes the correct parameters. As expected, when the EMF constant is increased, the torque capability increases in the constant torque operating range, the base speed reduces, and the flux-weakening performance deteriorates. In general, however, the motor parameters which are used in feedforward control algorithms will differ from the actual motor parameters, due to temperature and saturation variations, for example, which affect the stator winding resistance and the flux linkage and, in turn, the d- and q-axes inductances. Hence, the motor performance which is achieved with optimal I_d^* and I_q^* current profiles derived from such a model will be inferior, to a greater or lesser degree, to that which the motor is inherently capable of producing. Again, by way of example, Fig. 1(b) shows the sensitivity of the achievable

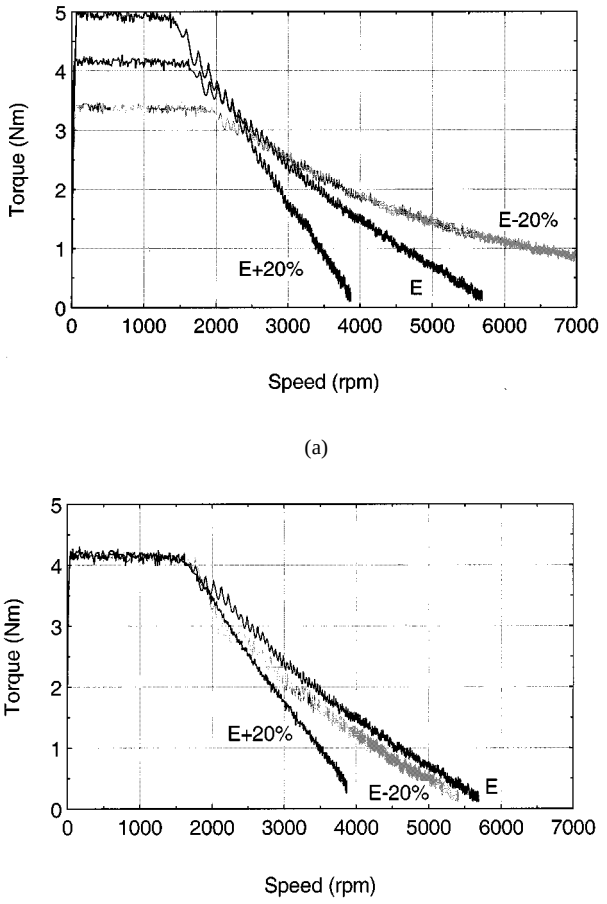

(a)

(B)

Fig. 1. Dependence of performance, achieved with feedforward control, on back-EMF constant E. (a) Effect of actual motor EMF. (b) Effect of EMF assumed in controller.

Paper IPCSD 00–027, presented at the 1999 IEEE International Electric Machines and Drives Conference, Seattle, WA, May 9–12, and approved for publication in the IEEE TRANSACTIONS ON INDUSTRY APPLICATIONS by the Electric Machines Committee of the IEEE Industry Applications Society. Manuscript submitted for review July 2, 1999 and released for publication June 21, 2000.

Z. Q. Zhu and D. Howe are with the Department of Electronic and Electrical Engineering, University of Sheffield, Sheffield S1 3JD, U.K. (e-mail: Z.Q.Zhu@sheffield.ac.uk; d.howe@sheffield.ac.uk).

Y. S. Chen was with the Department of Electronic and Electrical Engineering, University of Sheffield, Sheffield S1 3JD, U.K. He is now with the TRW Automotive Technical Center, Birmingham B90 4GW, U.K. (e-mail: Yang.Chen@TRW.com).

Publisher Item Identifier S 0093-9994(00)10425-6.

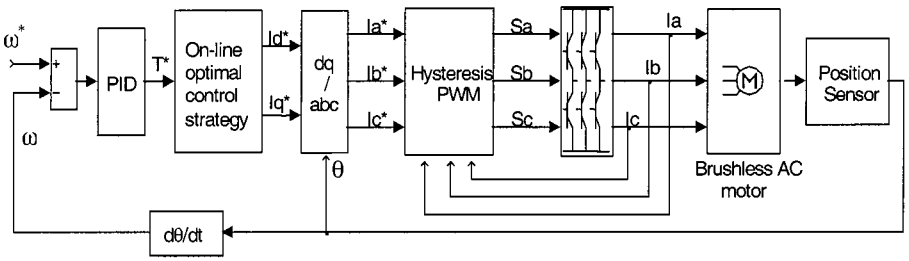

Fig. 2. Online optimal vector control of brushless ac drive.

torque–speed characteristic of the same brushless ac motor when the back-EMF constant which is assumed in the model differs from the actual value [9]. As will be seen, only the flux-weakening performance is compromised.

Since the predetermined optimal I_d^* and I_q^* current profiles are relatively sensitive to variations in the motor parameters, the use of an online optimal control strategy, which is independent of the parameters and always ensures that optimum performance is achieved over the entire speed range, may be desirable. This paper describes a comprehensive online optimal control strategy, which incorporates enhancements to previously published strategies [1]–[5], [11], and reports on the resulting steady-state and transient dynamic performance of typical brushless ac motors.

II. Online Optimal Flux-Weakening Control

Online optimal control was first applied to induction motors [10], in order to optimize the system efficiency. Subsequently, it was applied to open-loop-controlled permanent-magnet synchronous motors [11] and, more recently, to permanent-magnet brushless dc motors [12], the supply voltage/frequency ratio [11] or the commutation angle [12] being adjusted to minimize the dc-link current and, again, maximize efficiency. In this paper, online optimization is applied to vector-controlled permanent-magnet brushless ac drives, with particular reference to enhancing their flux-weakening performance.

The proposed control strategy is an extension to the strategies reported in [3] and [4], which are also independent of the motor parameters, and used either the error in the d-axis current $\Delta I_d = I_d^* - I_d$ [3] or the q-axis current $\Delta I_q = I_q^* - I_q$ [4] to modify I_d^* and I_q^*, for maximum torque per ampere [3], [5]. In the proposed strategy, the optimal values of I_d^* and I_q^* are searched online. However, when a significant change in either the demanded or the actual speed occurs, in order to improve the dynamic response, I_d^* and I_q^* are determined from optimal current profiles for maximum power operation, which are deduced as for the feedforward flux-weakening control described in [2]. When the motor reverts to steady-state operation, the values of I_d^* and I_q^* as determined from the optimal current profiles are used as initial values to accelerate the online search process. The dc-link current, the q-axis current error, and the speed are then used as optimization objectives during the online optimization, which ensures that the power capability is maximized over the complete operating range.

The online optimal flux-weakening control system is shown in Fig. 2, and is essentially the same as that given in [9], except that the optimal I_d^* and I_q^* currents are determined online, rather than being predetermined, by varying the demagnetizing current component I_d^* within the range $0 \rightarrow -I_{\max}$, where $I_{\max}$ is the rated phase current of the motor. The torque-producing current component I_q^* is determined by the demanded torque, but its maximum value is limited to $\sqrt{I_{\max}^2 - I_d^{*2}}$.

The flow chart of Fig. 3 illustrates the principle of the online optimization algorithm, as implemented on a fixed-point digital signal processor (DSP) (TMS320C50) which controls a hysteresis current-controlled insulated gate bipolar transistor (IGBT) inverter. It is relatively simple, in that the value of I_d^* is changed periodically by a variable increment ΔI_d^*, which is determined according to its effect on the performance of the drive. Essentially, if the motor performance improves after successive incremental changes in I_d^* of a given magnitude and polarity, the increment ΔI_d^* is automatically increased in magnitude, otherwise its polarity is changed and its magnitude reduced.

Since the changes which need to be made to I_d^* and $\Delta I_d^*$are dependent on the variation in the performance of the motor, a key issue is the assessment of this variation. The controller considers three operating scenarios, signified by *(1)–(3)* in Fig. 3.

Scenario (1):

$$I_q^* - I_q > I_{q\_\text{error}}.$$

This is unlikely to occur in the constant torque operating range for a well-designed and tuned control system. However, in the flux- weakening mode, if $|I_d|$ is less than the optimal value, I_q will be unable to attain the commanded value I_q^*, since it will be limited by the maximum inverter voltage. Therefore, if $I_q^* - I_q > I_{q\_\text{error}}$, where I_{q_error} is set to an appropriate value, I_d^* is optimized so as to maximize the output power and reduce the error $I_q^* - I_q$. Hence, the motor speed and $I_q^* - I_q$ are used as search criteria, by which to assess changes in the motor performance, either an increase of speed or a decrease of $I_q^* - I_q$ indicating an improvement.

Scenario (2):

$$I_q^* - I_q < I_{q\_\text{error}} \text{ and } I_a^* = \sqrt{I_d^{*2} + I_q^{*2}} < I_{\max}.$$

In this case, the motor operating point is within the maximum achievable torque/power-speed envelope. $I_q^*$is now determined by the demanded torque, while I_d^* is minimized online so as to

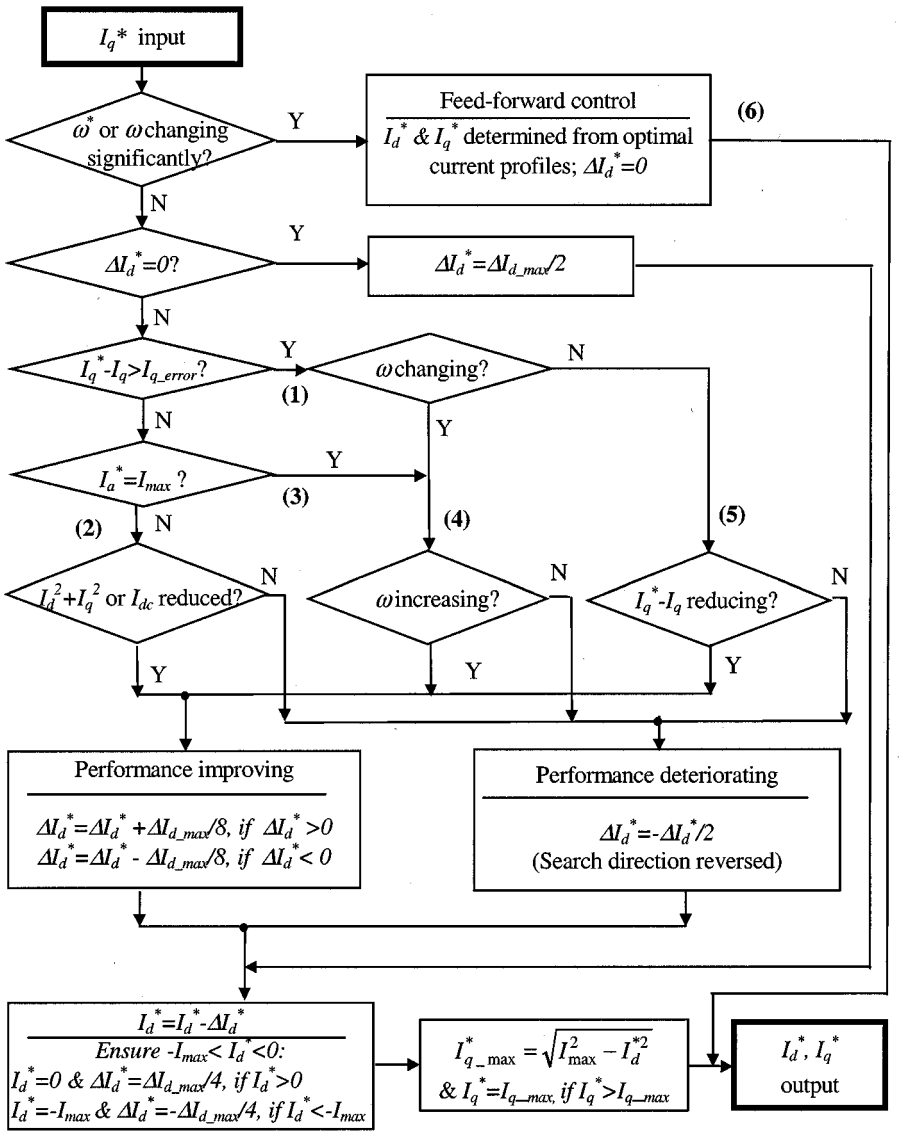

Fig. 3. Flow chart of online optimal control strategy.

reduce the motor phase current $I_a=\sqrt{I_d^2+I_q^2}$ or the dc-link current $I_{\rm dc}$. Minimum phase current results in minimum motor copper loss, while minimum dc-link current results in minimum input power, the output power being maintained by I_q. In Fig. 3, either the phase current $I_a=\sqrt{I_d^2+I_q^2}$ or the dc-link current $I_{\rm dc}$ is used as the search criteria. Below base speed, therefore, the control algorithm optimizes the motor performance for maximum torque-per-ampere phase current or maximum drive system efficiency. Above base speed, if the demagnetizing current $|I_d|$ was smaller than the optimal value, $I_q^*-I_q<I_{q\_\rm error}$ would not be possible. Hence, $|I_d|$ would be increased until it is equal to or larger than the optimal value. In other words, in the flux-weakening range, when $I_q^*-I_q<I_{q\_\rm error}$ the demagnetizing current $|I_d|$ is usually greater than the optimal value. Thus, the copper loss is increased, while the terminal voltage is not fully utilized, i.e., $U_a=\sqrt{U_d^2+U_q^2}<U_{\rm max}$, where U_a is the phase voltage and $U_{\rm max}$ is the maximum inverter voltage. Therefore, the motor performance will be automatically driven toward the optimal operating point, at which $U_a=\sqrt{U_d^2+U_q^2}=U_{\rm max}$ and I_d is a minimum.

Scenario (3):

$$I_a^*=\sqrt{I_d^{*2}+I_q^{*2}}=I_{\rm max}.$$

In this case, the demanded motor operating point is along the maximum torque/power-speed characteristic. Due to the inverter voltage limit, however, an incorrect ratio of I_d^*/I_q^* will cause the actual values of I_d and/or I_q to be lower than the demanded values. Therefore, $I_a=\sqrt{I_d^2+I_q^2}<I_{\rm max}$. The optimal ratio of I_d^*/I_q^* is that which maximizes the motor output power, for the maximum rated phase current $I_{\rm max}$. Hence, the dc-link current may again be used as the optimization criteria,

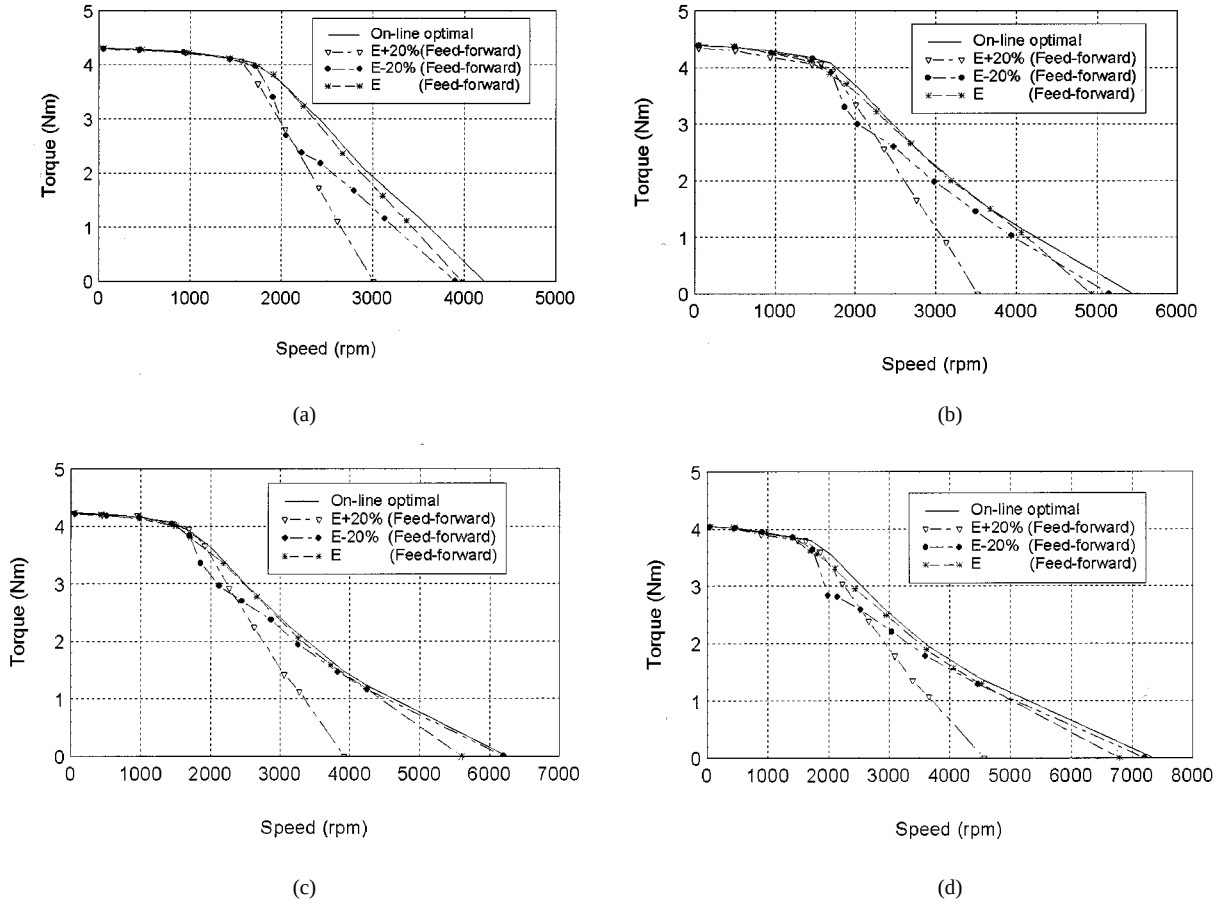

Fig. 4. Measured maximum torque–speed curve of brushless ac motors with alternative rotor topologies. (a) Surface-mounted magnet. (b) Inset magnet. (c) Interior radial magnet. (d) Interior circumferential magnet.

but with I_d^* now being varied to maximize the dc-link current and, therefore, the motor input power. However, since I_q^* is determined by $\sqrt{I_{\max}^2 - I_d^{*2}}$, and may be less than the value which is required by the demanded torque, the speed error $\omega^* - \omega$ may increase. Hence, as shown in Fig. 3, the optimal I_d^* is online searched and the speed ω is used as the optimization criteria, since an increase in ω signifies an increase of output power.

Existing control strategies essentially correspond to the various operating regimes which are signified as *(1)–(6)* in Fig. 3. For example, the maximum efficiency control strategies, which are described in [2], [11], and [12], correspond to operating regime *(2)* in Fig. 3, in which the dc-link current is minimized; the flux-weakening control strategies, which are based on current feedback, as described in [3] and [4], correspond to operating regime *(5)* in Fig. 3, while the flux-weakening control strategies, which are based on feed-forward control of the optimal current profiles as described in [1], [2], and [9], correspond to operating regime *(6)* in Fig. 3. However, none of the existing control strategies use the motor speed as one of the optimization objectives, as in operating regime *(4)* in Fig. 3. As mentioned earlier, in order to fully utilize the voltampere rating of the inverter, as in scenario *(3)* in Fig. 3, the dc-link current is maximized, which is the opposite of scenario *(2)*. In addition, the maximum power capability, which is achieved with a maximum efficiency control strategy, is always somewhat inferior to that of which the motor is inherently capable. The proposed online optimal control always ensures that the maximum inherent power capability of the motor is achieved, and then seeks to maximize the efficiency.

III. Experimental Results of Steady-State and Transient Dynamic Performance

The online optimal control algorithm has been applied to four brushless ac motors, having interior (radial or circumferential), inset, and surface-mounted magnet rotors, for which design details are given in the Appendix. Fig. 4 compares the measured maximum torque–speed curve which is achieved with the online optimal control strategy with that which is obtained with conventional feedforward control, based on measured motor parameters [9]. As will be seen, the online control strategy results in slightly better performance over the high-speed operating range. However, in order to highlight that the performance of feedforward control is sensitive to the assumed motor parameters, Fig. 4 also includes measured maximum torque–speed curves which result when the assumed back-EMF constant differs from the measured value. As can be seen, with online optimal control all the motors achieve their maximum inherent performance capability, and eliminate the influence of errors in the motor parameters, i.e., the steady-state performance is always better than that which is obtained with feedforward control.

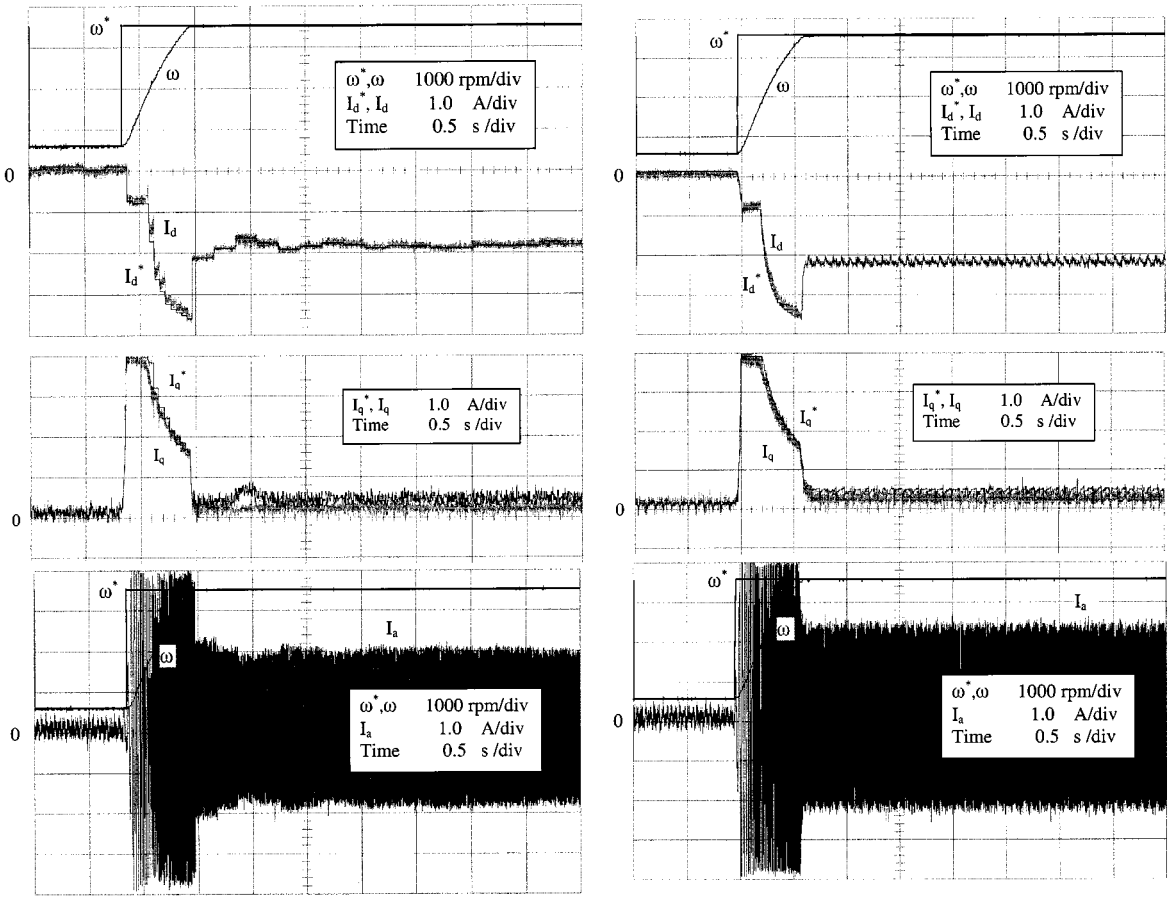

Fig. 5. Variation of demanded and actual d–q-axis phase currents during commanded speed change. (a) Online optimal control (time step $=200$ ms) with optimal current profile control regime (time step $=50$ ms). (b) Feedforward control.

In order to illustrate the transient dynamic performance of the online optimal algorithm, Fig. 5(a) compares the variation of the demanded d- and q-axes currents I_d^* and I_q^* with the actual currents I_d and I_q of the brushless ac motor having an interior radial magnet rotor, following a step change in the commanded speed, from 500 r/min in the constant torque range to 3500 r/min in the flux-weakening range, i.e., about two times base speed. By way of comparison, Fig. 5(b) shows the response with feedforward control, in which I_d^* is initially maintained constant for maximum torque per ampere up to base speed, after which I_d^* and I_q^* follow predetermined optimal current profiles for flux-weakening operation. As long as the demanded operating working point is within the maximum power capability which is achievable with this control strategy, I_d and I_q follow the demanded profiles quite well. Hence, the response is good, and the motor quickly attains steady state. Clearly, if the demanded operating working point is beyond the maximum achievable power capability, but within the inherent power capability, the dynamic performance will deteriorate and the demanded working point will not be attained.

With the proposed online optimal control, the algorithm reverts to feedforward control whenever the rate of speed change exceeds a prescribed value. Thus, since there are significant variations in the commanded and actual speeds, the initial control strategy is also feedforward, I_d^* being maintained constant initially in the constant torque range before following the optimal current profiles in the constant power range, both corresponding to maximum torque per ampere. However, the average performance, i.e., the average speed in this case, is monitored continuously over fixed time steps (50 ms, ≈200 sampling points), and once the steady state has been attained, online optimal control is implemented, and the average performance is monitored over longer time steps (200 ms, ≈1000 sampling points). Thus, I_d^* and I_q^* change automatically in magnitude, and in variable increments, as the commanded speed is approached, at which time I_d^* and I_q^* have attained optimal values. Comparing Fig. 5(a) and (b), it can be seen that online optimal control has retained the good transient dynamic performance of feedforward control, but has the advantages of enhanced maximum torque/power capability and improved efficiency (lower phase current), particularly in the flux-weakening operating range.

In order to further highlight the performance improvement which is achieved with the online optimal control algorithm, the step response which results from an online search alone, i.e., without the feedforward control regime, and which results from the online optimal control strategy using a constant time step are shown in Fig. 5(c) and (d), respectively. It will be observed that the demanded d-axis current in Fig. 5(c) is initially set to zero

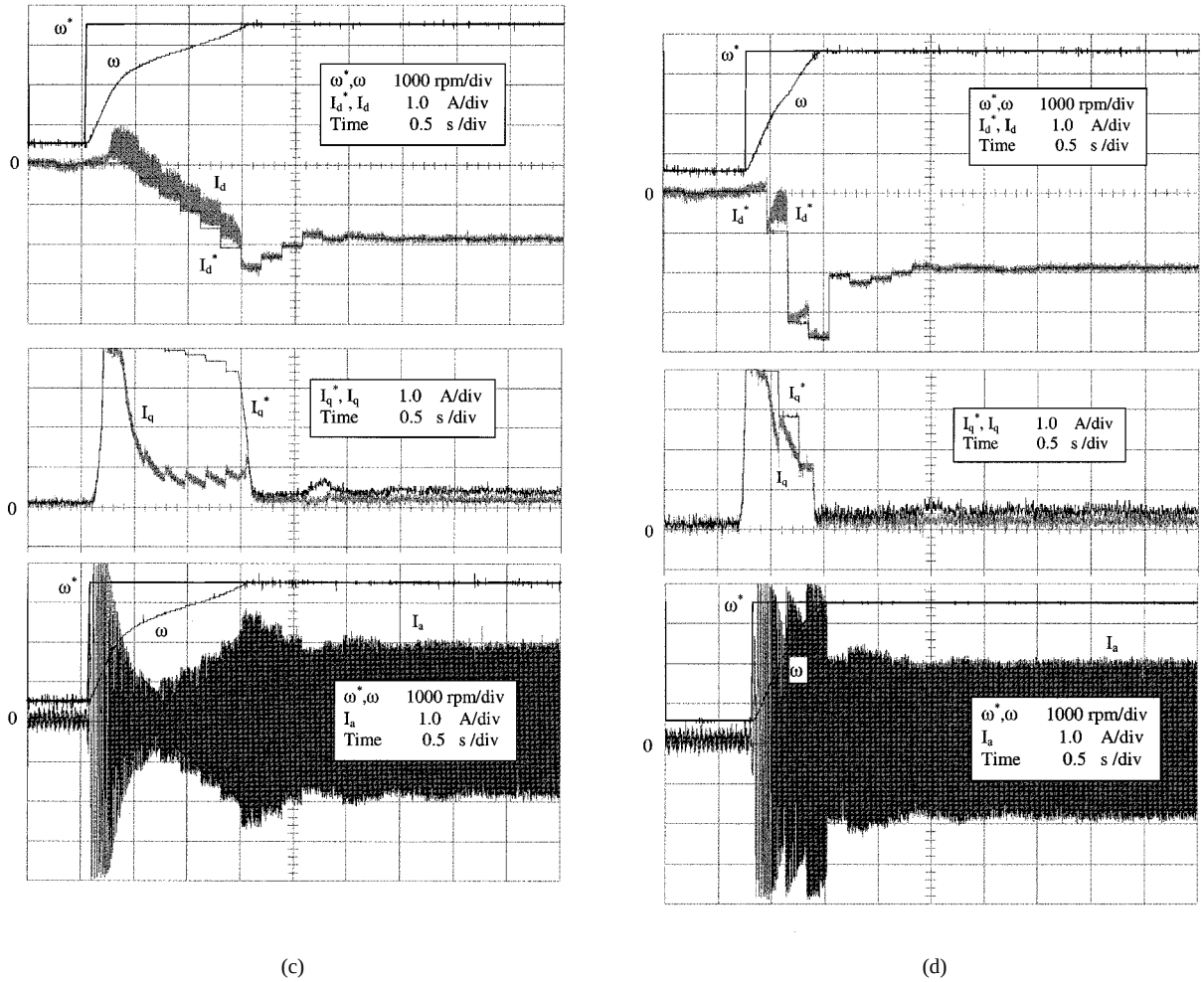

(c) (d)

Fig. 5. *(Continued.)* Variation of demanded and actual d–q-axis, phase currents during commanded speed change. (c) Online optimal control without optimal current profile control regime (time step $=$ 200 ms). (d) Online optimal control (time step $=$ 200 ms) with optimal current profile control regime (time step $=$ 200 ms).

until the speed variation is within the specified band, which has deliberately been set large so that the optimal search starts when the actual speed reaches about 2/3 of the commanded speed. However, the online search for the optimal I_d^* is not sufficiently fast to follow the commanded change in speed. Consequently, when the motor enters the flux-weakening range the actual q-axis current cannot follow the demanded current due to the converter voltage limit. As a result, the step response is very slow and much inferior to that which is obtained with feedforward control. One possible way of improving the dynamic performance is to reduce the time step when searching for the optimal I_d^*. However, the resulting improvement has been found to be rather limited, while undesirable oscillations may occur if the time-step length is too small. Fig. 5(d) again shows the improved step response which results when feedforward control is integrated into the online optimal control algorithm, I_d^* and I_q^* being set to values deduced from optimal current profiles when there is a significant change in either the commanded or actual speed. However, due to the use of identical time steps during both transient and steady-state operation, the q-axis current exhibits an error during the transient period when the feedforward optimal current profile control is employed. To reduce this current error, the time step during the transient may be reduced, as was the case in Fig. 5(a).

IV. Conclusions

An improved online optimal control strategy has been developed, and applied to alternative permanent-magnet brushless ac motor topologies. The dc-link current, the q-axis current error, and the speed are used as optimization objectives, according to different operating scenarios. In addition, since it is coupled with feedforward vector control, based on optimal current profiles, it retains excellent transient dynamic performance, while achieving the maximum inherent power capability of the motor in the flux-weakening range and guaranteeing maximum efficiency over the entire operating range.

Appendix

Four prototype three-phase six-pole brushless permanent-magnet ac motors were used during the investigation. As shown in Fig. 6, they have the same stator design but different rotors: surface-mounted magnet, inset magnet, and interior (radial or circumferential) magnet, the ratio of $\omega L_d I_{\max}/E$

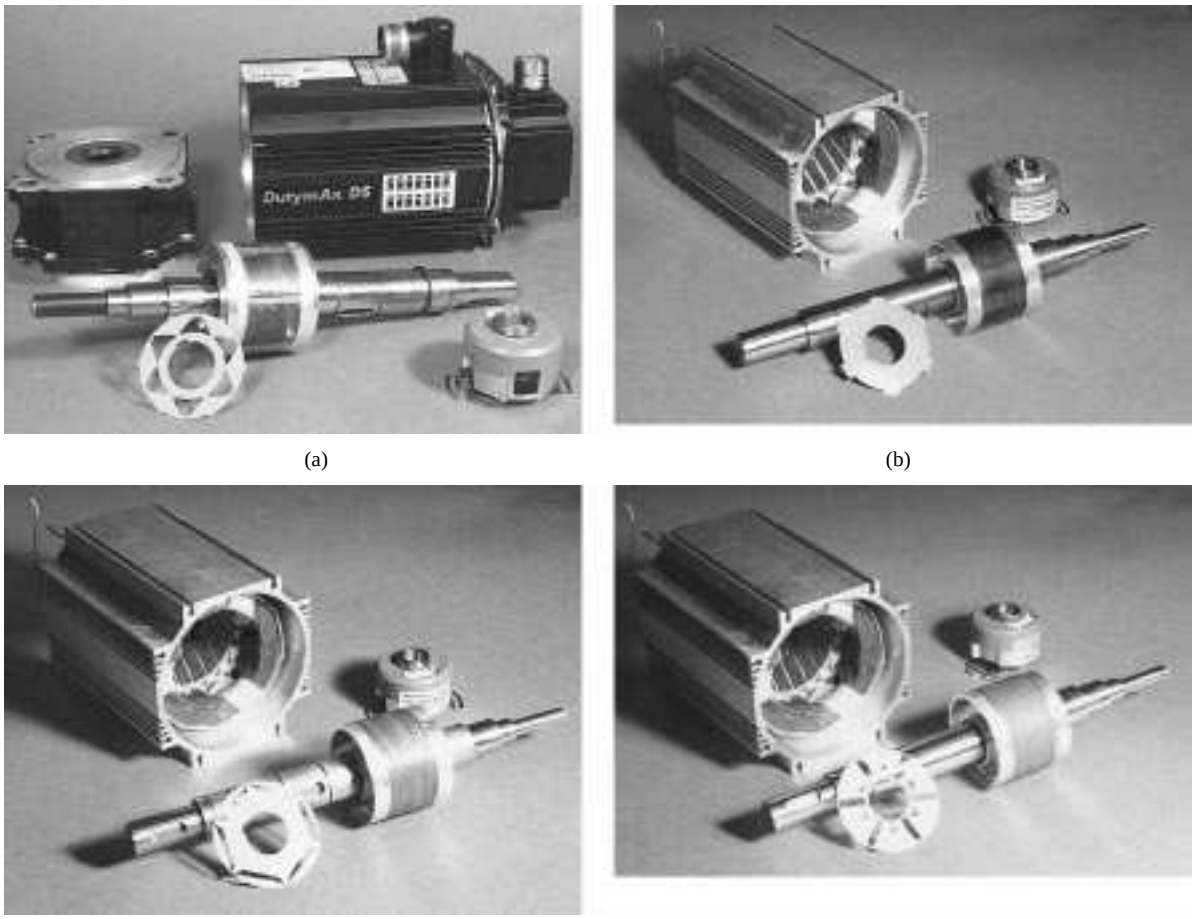

Fig. 6. Brushless ac motors with different rotor topologies. (a) Surface-mounted magnet. (b) Inset magnet. (c) Interior radial magnet. (d) Interior circumferential magnet

being 0.45, 0.57, 0.61, and 0.69, respectively. The dc-link voltage $U_{\rm dc} = 285$ V, the rated phase current $I_{\max} = 4$ A (peak), and the base speed ≈1700 r/min.

REFERENCES

[1] S. Morimoto, Y. Takeda, and T. Hirasa, "Current phase control methods for permanent magnet synchronous motors," *IEEE Trans. Power Electronics*, vol. 5, pp. 133–139, Apr. 1990.

[2] S. Morimoto, M. Sanada, and Y. Takeda, "Wide-speed operation of interior permanent magnet synchronous motors with high-performance current regulator," *IEEE Trans. Ind. Applicat.*, vol. 30, pp. 920–926, July/Aug. 1994.

[3] T. M. Jahns, "Flux-weakening regime operation of an interior permanent magnet synchronous motor drive," *IEEE Trans. Ind. Applicat.*, vol. IA-23, pp. 681–689, July/Aug. 1987.

[4] S. D. Sudhoff, K. A. Corzine, and H. J. Hegner, "A flux-weakening strategy for current-regulated surface-mounted permanent-magnet machine drives," *IEEE Trans. Energy Conversion*, vol. 10, pp. 431–437, Sept. 1995.

[5] T. M. Jahns, G. B. Kliman, and T. W. Neumann, "Interior permanent-magnet synchronous motors for adjustable-speed drives," *IEEE Trans. Ind. Applicat.*, vol. IA-22, pp. 738–747, July/Aug. 1986.

[6] J. M. Kim and S. K. Sul, "Speed control of interior permanent magnet synchronous motor drive for the flux weakening operation," *IEEE Trans. Ind. Applicat.*, vol. 33, pp. 43–48, Jan./Feb. 1997.

[7] R. F. Schiferl and T. A. Lipo, "Power capability of salient pole permanent magnet synchronous motors in variable speed drive application," *IEEE Trans. Ind. Applicat.*, vol. 26, pp. 115–123, Jan./Feb. 1990.

[8] W. L. Soong and T. J. E. Miller, "Field-weakening performance of brushless synchronous AC motor drives," *Proc. IEE—Elect. Power Applicat.*, vol. 141, pp. 331–340, Nov. 1994.

[9] Y. S. Chen, Z. Q. Zhu, and D. Howe, "Influence of inaccurancies in machine parameters on the flux-weakening performance of permanent magnet brushless ac drives," in *Proc. IEMDC99*, 1999, pp. 691–693.

[10] D. S. Kirschen, D. W. Novotny, and T. A. Lipo, "On-line efficiency optimization of a variable frequency induction motor drive," *IEEE Trans. Ind. Applicat.*, vol. IA-21, pp. 610–615, May/June 1985.

[11] R. S. Colby and D. W. Novotny, "An efficiency-optimizing permanent-magnet synchronous motor drive," *IEEE Trans. Ind. Applicat.*, vol. 24, pp. 462–469, May/June 1988.

[12] C. C. Chan, W. Xia, J. Z. Jiang, K. T. Chau, and M. L. Zhu, "Permanent magnet brushless drives," *IEEE Ind. Applicat. Mag.*, vol. 4, pp. 16–22, Nov./Dec. 1998.

Z. Q. Zhu (M'90) received the B.Eng. and M.Sc. degrees from Zhejiang University, Hangzhou, China, and the Ph.D. degree from the University of Sheffield, Sheffield, U.K., in 1982, 1984, and 1991, respectively, all in electrical and electronic engineering.

From 1984 to 1988, he was a Lecturer in the Department of Electrical Engineering, Zhejiang University. Since 1988, he has been with the University of Sheffield, where he is currently a Senior Research Scientist in the Department of Electronic and Electrical Engineering. From 1999 to 2000, he was a Visiting Professor at the University of Hong Kong. He is also an Advisory Professor at Shanghai University. His major research interests include the application, control, and design of permanent-magnet machines and drives. He has authored more than 130 published journal and conference papers.

Dr. Zhu is a Chartered Engineer in the U.K. and a member of the Institution of Electrical Engineers, U.K.

Y. S. Chen received the B.Eng and M.Sc. degrees from Zhejiang University, Hangzhou, China, and the Ph.D. degree from the University of Sheffield, Sheffield, U.K., in 1991, 1994, and 2000, respectively, all in electrical and electronic engineering.

From 1994 to 1995, he was a Research Engineer with the Computer Periphery Research Institute, China, and from 1999 to 2000, he was an Electronics Engineer with Control Techniques Dynamics Ltd., U.K. Since 2000, he has been with the TRW Automotive Technical Center, Birmingham, U.K., as an Electric Actuation Engineer. His research interests are electrical machines and drives.

David Howe received the B.Tech. and M.Sc. degrees from the University of Bradford, Bradford, U.K., and the Ph.D. degree from the University of Southampton, Southampton, U.K., in 1966, 1967, and 1974, respectively, all in power engineering.

He has held academic posts at Brunel and Southampton Universities, and spent a period in industry with NEI Parsons Ltd., working on electromagnetic problems related to turbogenerators. He is currently Lucas Professor of Electrical Engineering at the University of Sheffield, Sheffield, U.K., where he heads the Electrical Machines and Drives Research Group. His research activities span all facets of controlled electrical drive systems, with particular emphasis on permanent-magnet excited machines. He is the author of more than 200 publications in the fields of machines, drives, and motion control systems.

Prof. Howe is a Chartered Engineer in the U.K. and a Fellow of the Institution of Electrical Engineers, U.K.